PREDICTION OF NEW ETCH FRONTS IN BLACK SILICON PRODUCED BY CRYOGENIC DEEP REACTIVE ION ETCHING

D. Abi-Saab[1], P. Basset[1], M. J. Pierotti[2], M. L. Trawick[2] and D. E. Angelescu[1]
[1]Université Paris-Est, ESIEE Paris, ESYCOM, 93162 Noisy le Grand, France
[2]University of Richmond, Richmond, 23173 Virginia, USA

ABSTRACT

This paper presents an explanation of the dynamic formation of black silicon (BSi) during deep reactive ion etching (DRIE) processes which has been confirmed by both experimental data with cryogenic DRIE and computational modeling. The model described the strong dependence of the substrate topography on the etching parameters and its evolution with process time. It shows the importance of the self-shadowing effect on the final structures and allows predicting the most important aspects of the BSi phenomenology such as the new etching fronts appearing at topographical saddle points during the incipient stages of BSi development.

KEYWORDS

Black silicon, reactive ion etching, DRIE, nanostructure, modelling.

INTRODUCTION

Black Silicon (BSi) is an artificially produced dark material resulting from the submicro/nano-structuration of a crystalline silicon (Si) surface. These micro/nano-structures change the behavior of the light reaching the surface by making multiple reflections and interferences and so greatly reducing the surface reflectance. This makes the silicon surface to look black to the eye [1]. It can also be either superhydrophobic or superhydrophilic by adding a conformal layer of perfluorinated polymers or silicon dioxide [2].

The maskless BSi fabrication method by plasma etching comprises the continuous reactive ion etching at cryogenic temperatures (cryo-DRIE) [3] and the time-multiplexed reactive ion etching at room temperature (Bosch process) [4]. In addition, BSi can be fabricated using a wet etching combined with a nanoparticles deposition step [5] or laser-chemical etching [6].

Maskless BSi formation by DRIE is not yet well understood. Initial hypothesis attributed the BSi formation to micromasking due to native oxide of the Si wafer [3][7]. Recently BSi formation has been attributed to polymeric nano-masking appearing at the beginning of the DRIE process [9]. Previous models have been proposed using a shadowing factor and a sticking coefficient in order to predict the evolution of roughness observed in conventional reactive ion etching processes [8] or based on quantum mechanics and diffusion theory [9].

In order to better understand the BSi topography formation, we have developed a novel BSi topographical characterization technique which is based on in-plane focused ion beam nanotomography. It can reproduce silicon nanostrucures with any aspect ratio and sample details with accuracy of 10 nm. Then, we developed an experimentally-backed phenomenological model that is capable of simulating the entire evolution of a surface from a planar substrate to fully developed BSi topography. We produce phase diagrams which captures the parameter combinations responsible for BSi formation. We also observe experimentally and are able to reproduce, within our model, a number of subtle effects that leads to the observed pattern densification that is responsible for BSi formation during DRIE.

BLACK SILICON 3D RECONSTRUCTION

We proceed to the three-dimensional reconstruction using Focused Ion Beam (FIB) nanotomography of one BSi sample (labelled S01 and fabricated by cryo-DRIE). This technique consists in introducing the BSi sample in a dual beam microscope. Conventional positioning of the BSi sample in the dual beam microscope requires the deposition of a contrast enhancement layer (usually platinum) in order to facilitate the boundary detection between etched and non-etched material [7]. We proposed to place the BSi sample in-plane to the FIB beam (as illustrated in Fig. 1). This beam makes sequential cuts of the BSi and the electron beam takes cross section images between each cut. The advantage of the in-plane positioning of the BSi sample is that it does not require applying a contrast enhancement layer, because the SEM beam being closer to the sample's top-view provides sufficient contrast for direct edge detection.

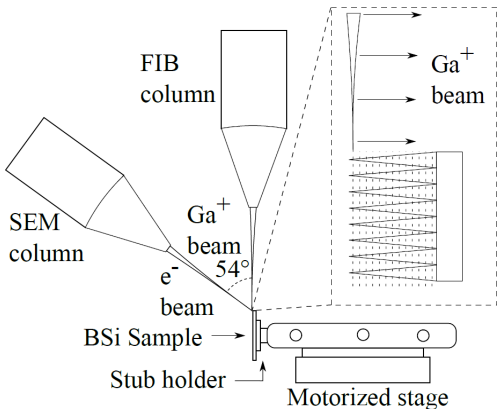

Figure 1: Diagram of in-plane BSi positioning in a dual beam FIB-SEM microscope.

Once all these cross-section SEM images are obtained from the FIB nanotomography process, we perform a series of image treatment techniques, allowing to obtain a three dimensional representation of the BSi surface. The data processing includes the registration of the SEM images to correct the sample movements and drift during the FIB nanotomography process. We then proceed to a subtraction of the SEM images taken with different detectors in order to remove the features that may interfere with the detection of the boundary between etched and non-etched Silicon. We proceed to an image rescaling in order to obtain the top view aspect ratio of the structures and the edge detection. Finally we calculate the elevation of each SEM image slice. With a Delaunay triangulation of the edge information in each slice, we obtain a three dimensional representation of the BSi surface. We compare the three dimensional reconstruction with SEM images taken previously with the FIB analysis. It shows an accurate reconstruction with a resolution in the order of 10 nm (Figure 2). This analysis also shows that the BSi surface consists of a network of connected holes with some peak structures that are the result of the intersection of these holes.

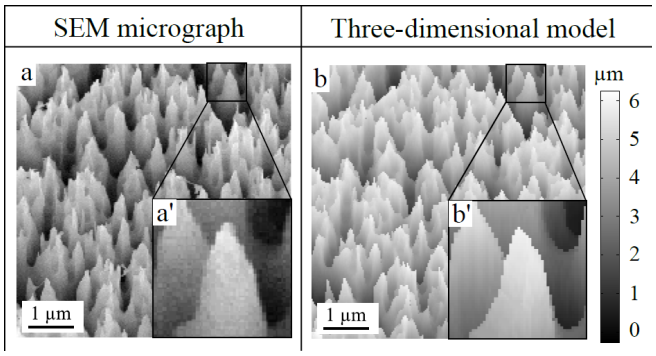

Figure 2: 20° tilt view of BSi sample S01: (a and a') SEM micrograph, (b and b') three-dimensional reconstruction.

BSI FORMATION MECHANISMS

In order to obtain more information on the BSi structures formation during the process, we proposed a time-lapse etching experiment with a combination of small period etching steps and SEM imaging showing in the same region the topographical changes from a planar surface to the final BSi structures.

In this model (and also experimental data as we will show later) the initial flat surface of the Si sample is unstable to hole's formation, because the passivation layer etching (due to plasma's ions) is anisotropic, and so it is equally strong on top of peaks and bottom of holes. Then we have two zones with different etching behavior (see Figure 3). Firstly, the areas where the passivation layer formation is absent due to occlusion at the bottom of the holes, so the silicon etching tends to be higher. Secondly, the areas on top of peaks which are over-passivated due the high exposure to the radical diffusion of gases leading to the passivation layer growth (essentially the oxygen radical in the case of cry-DRIE). So the effective etching condition is slower or there is no silicon etching at all. Once we have some initial structures formed from the initial roughness of the silicon sample, we observe a third zone on saddle areas where the passivation formation and etching rates are balanced so the silicon etching is high, allowing the formation of new etch fronts.

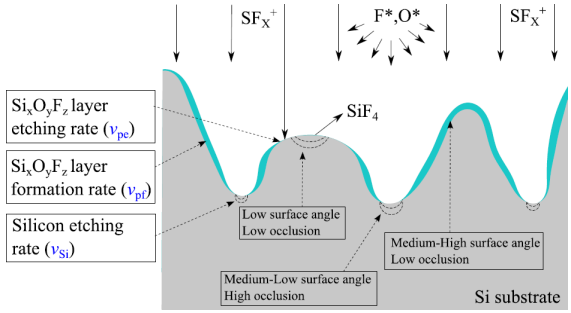

Figure 3: Principle of maskless BSi formation mechanisms using plasma etching. Illustration for cryo-DRIE process.

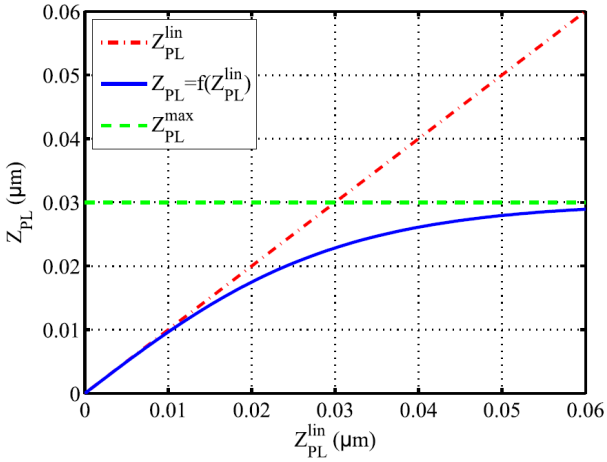

Figure 4: Actual passivation layer thickness Z_{PL} vs. calculated passivation layer thickness in the cryo-DRIE process $Z^{lin}_{PL,}$ assuming linear growth. The red line represents the linear growth without self-limiting process. The blue line represents the actual growth taking into account a self-limiting process to a predefined maximum passivation thickness Z^{max}_{PL} (green line).

In our model, we start by introducing the initial substrate which can be a polished silicon wafer with nanoscale initial roughness or a surface that have already tridimensional structures. We setup the model parameters such as maximum passivation formation rate (v_{pf}), maximum passivation etching rate (v_{pe}), maximum silicon etching rate (v_{Si}) and process time (t_{proc}). Then we simulate the deep reactive ion etching process with the following steps: (1) the passivation layer formation based on the occlusion level of the surface, (2) the passivation layer etching based on the surface normal angle and (3) the silicon etching also based on occlusion level [10]. Then the process is repeated until we reach the required process time. For cryo-DRIE which is a continuous process, these three steps of the model are discretized in very small fraction of

time.

In addition to the occlusion level, one of the important features that we included in the model is the self-limiting mechanism in the passivation layer formation rate. Since the passivation layer thickness increases with time, it is more difficult, in cryo-DRIE, for the oxygen and fluorine radicals to interact with the silicon. So we introduced a sigmoid function (c.f. Figure 4) where the actual passivation thickness is calculated assuming a linear growth and a maximum passivation thickness.

Thanks to our model, we can determine phase diagrams of the silicon etch depth dependence with the simulation parameters. In Figure 5 we show a section of the phase diagram based on the passivation formation rate (which can be related to the oxygen content for cryo-DRIE) and the passivation etching rate (which can be related to the voltage bias). In this phase diagram we can observe a transition from no etching when we have a high v_{pe} down to a uniform etching when v_{pe} is increased. We also observe in the middle of this transition the formation of high aspect ratio structures similar to those obtained in black silicon samples.

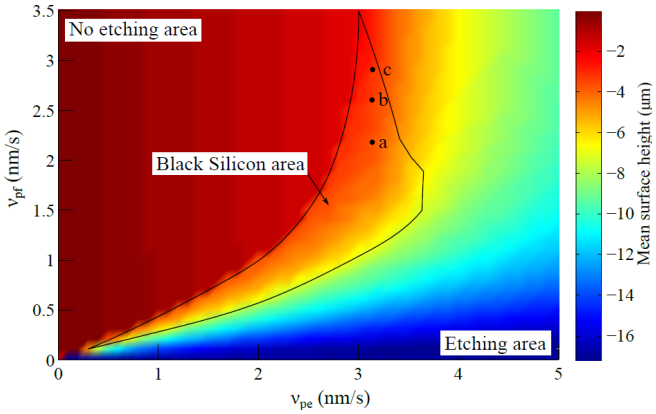

Figure 5: Diagram of Silicon etch depth dependence on v_{pe} and v_{pf}, the other parameters being fixed (v_{Si} = 30 nm/s and t_{proc} = 10 minutes).

The black silicon zone is similar to the ones described previously in the so called black silicon method which was proposed in the early stage of silicon etching with reactive ions [11]. This method has been used for an easy calibration of the RIE apparatus parameters to obtain a perfectly vertical silicon etching profile. This phase diagram also suggests that there is a possibility of a transition between no etching to uniform etching without passing the black silicon region.

We calculate the aspect ratio of the simulated structures at different passivation formation rate values and with a fixed value of passivation etching rate. We compared them to BSi samples previously fabricated at different oxygen flow by cryo-DRIE [12]. A decrease in the structure aspect ratio is found in the simulations when the passivation formation rate is increased [10] and it is also observed in the experimental data.

As an additional experiment, in Figure 6 we illustrate the BSi formation with process time starting from a polished Si wafer. The initial Si surface used in the experiment (Fig. 6a) is based on measurements of the roughness of polished silicon wafers made with atomic force microscopy. When the simulation is initialized, we first notice the formation of holes in Fig. 6b. These holes then rapidly etch and combine to form larger holes and trenches (Fig. 6c). We then observe that the difference in the etching speed between the highly occluded areas and the highly exposed areas allows the formation of the high aspect ratio structures (Fig. 6d). Finally, the etching speed tends to stabilize because of the highly occluded regions and the absence of planar surfaces.

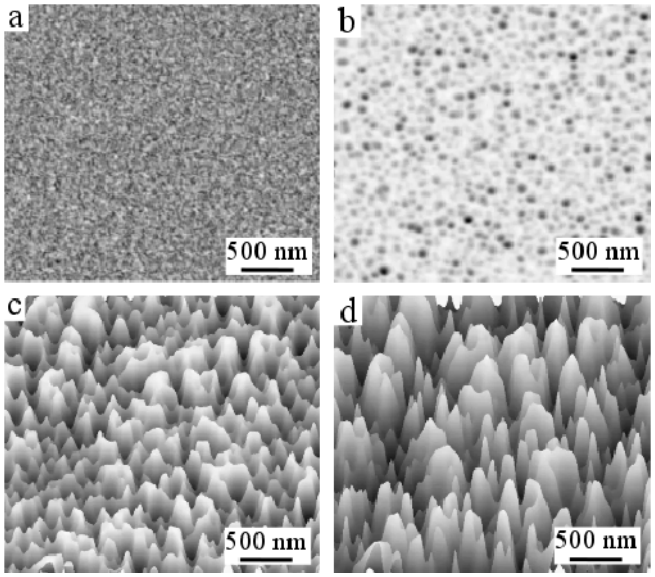

Figure 6: Dynamic study of BSi evolution with time. Simulation parameters: v_{pf} = 3.1 nm/s, v_{pe} = 3 nm/s and v_{Si} = 30 nm/s. t = 0 min. (a), t = 2 min. (b), t = 4 min (c) and t = 6 min. (d)

In the next study, we simulate the black silicon formation on surfaces which already has preexisting nanostructured, using the data obtained from time-lapse experiments. This allows us to predict the evolution of the black silicon topography and directly compare the results with real BSi samples. In order to introduce the initial topography into the simulation program, we use a non-destructive three dimensional reconstruction of the BSi sample. This reconstruction method is based on the analysis of the grayscale of a top view SEM image to convert it to a height map, similarly to the technique presented in [13]. Even though this technique has some limitations on BSi samples with high aspect ratio due to the SEM limited dynamical range, it is suitable for moderate aspect ratios such as the initial time-lapse samples used in our experiment. Figures 7a and 7b presents a 20° tilted SEM micrograph of the initial time-lapsed BSi sample (labelled S02) at t = 2 min. and the three-dimensional reconstruction using the gray scale analysis, respectively.

We then introduce the three-dimensional representation

of the time-lapse at t = 2 min. in the simulation program for one minute to obtain the sample prediction at t = 3 min. (Figure 7d). Finally, we compare the simulation results with the BSi sample obtained experimentally (Figure 7c). We observe in the simulation the same etching behavior when compared to the experimental data, including the formation of new etch fronts on top of preexisting structures, like those highlighted with circles.

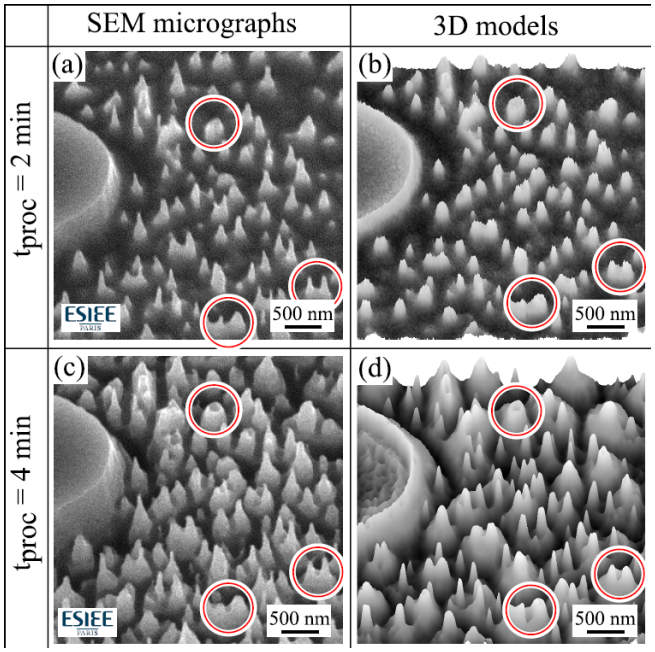

Figure 7: Time-lapse data showing the evolution of sample S02 between t = 2 min and t = 4 min of process time, for both simulation and experiment. 20° tilted view of: (a) initial time-lapse SEM and (b) three-dimensional reconstruction; (c) final time-lapse SEM (Temperature = -120°C, ICP power = 1000 W, bias voltage = -10 V, O_2 flow = 40 sccm, SF6 flow = 200 sccm and pressure = 1.5 Pa) and (d) final time-lapse simulation (v_{pf} = 2.5 nm/s, v_{pe} = 3 nm/s and v_{Si} = 30 nm/s). New etch fronts at topographical saddle points are highlighted with circles.

In conclusion, we have developed a model that is capable to simulate the black silicon formation by including the long range effects of the geometric occlusion. This model is capable to simulate different behaviors that were observed experimentally, such as the combination of the parameters that give rise to black silicon formation and their effect in the final aspect ratio, the dynamical change of the topography with the process time and the formation of new etch fronts on top of preexisting structures.

ACKNOWLEDGEMENTS

The author would like to thanks Professor Tarik Bourouina for useful discussions.

REFERENCES

[1] R. Dussart, X. Mellhaoui, T. Tillocher, P. Lefaucheux, M. Volatier, C. Socquet-Clerc, P. Brault, and P. Ranson, "Silicon columnar microstructures induced by an SF6/O2 plasma", *Journal of Physics D: Applied Physics*, 38, 18 (2005).

[2] V. Jokinen, L. Sainiemi, and S. Franssila, "Complex droplets on chemically modified silicon nanograss", *Advanced Materials*, 20, 18 (2008).

[3] G. Kumaravelu, M. Alkaisi and A. Bittar, "Surface texturing for silicon solar cells using reactive ion etching technique", *Proc. of the 29th Photovoltaic Specialists Conf.*, New Orleans (2002), pp. 258-261.

[4] C. Lee, S. Y. Bae, S. Mobasser and H. Manohara, "A novel silicon nanotips antireflection surface for the micro sun sensor", *Nano letters*, 5, 12 (2005).

[5] H. M. Branz, V. E. Yost, S. Ward, K. M. Jones, B. To and P. Stradins, "Nanostructured black silicon and the optical reflectance of graded-density surfaces", *Applied Physics Letters*, 94, 23 (2009).

[6] T.-H. Her, R. J. Finlay, C. Wu, S. Deliwala and E. Mazur, "Microstructuring of silicon with femtosecond laser pulses", *Applied Physics Letters*, 73, 12 (1998).

[7] M. Kroll, T. Käsebier, M. Otto, R. Salzer, R. Wehrspohn, E.-B. Kley, A. Tünnermann and T. Pertsch, "Optical modeling of needle like silicon surfaces produced by an ICP-RIE process", *Proc. of the SPIE Photonics for Solar Energy Systems III*, Brussels (2010), pp. 772505 - 772510.

[8] J. T. Drotar, Y.-P. Zhao, T.-M. Lu and G.-C. Wang, "Surface roughening in shadowing growth and etching in 2 + 1 dimensions", *Physical Review B*, 62, 3 (2000).

[9] F. Zhu, C. Wang, X. Zhang, X. Zhao and H. X. Zhang, "A three-step model of black silicon formation in deep reactive ion etching process", *Proc. of IEEE MEMS'2015*, pp. 365-368, 2015

[10] D. Abi-Saab, P. Basset, M. J. Pierotti, M. L. Trawick and D. E. Angelescu, "Satic and dynamic aspects of black silicon formation", *Physical Review Letter*, 113, 265502 (2014)

[11] H. Jansen, M. de Boer, R. Legtenberg and M. Elwenspoek, "The black silicon method: a universal method for determining the parameter setting of a fluorine-based reactive ion etcher in deep silicon trench etching with profile control", *Journal of Micromechanics and Microengineering*, 5, 2 (1995).

[12] K. Nguyen, P. Basset, F. Marty, Y. Leprince-Wang and T. Bourouina, "On the optical and morphological properties of microstructured black silicon obtained by cryogenic-enhanced plasma reactive ion etching", *Journal of Applied Physics*, 113, 19 (2013).

[13] F.-Y. Zhu, Q.-Q. Wang, X.-S. Zhang, W. Hu, X. Zhao, and H.-X. Zhang, "3D nanostructure reconstruction based on the SEM imaging principle, and applications", *Nanotechnology*, 25, 18 (2014).

CONTACT

* D. E. Angelescu, dan.angelescu@esiee.fr